A diffusing vortex model of a waterspout

P. G. BELLAMY-KNIGHTS (MANCHESTER) and L. HATTON (SURREY)

A CLASS OF UNSTEADY multicellular viscous vortex similarity solutions, which qualitatively agree quite well with the observed properties of waterspouts, is described and represented analytically by inner and outer series expansions. This solution is not externally driven in that there is no imposed axial pressure gradient. The highest order terms in the far field correspond to steady flow and the velocity tends to zero with increasing radial distance from the viscous core of the vortex.

Przedyskutowano klasę wielokomórkowych lepkich rozwiązań wirowych, które pod względem jakościowym dobrze opisują zachowanie się trąby wodnej; rozwiązania przedstawiono analitycznie za pomocą rozwinięć zewnętrznych i wewnętrznych. Przyjęto, że w przepływie otaczającym nie występuje osiowy gradient ciśnienia. Człony wyższego rzędu opisujące przepływ w dużej odległości od wiru odpowiadają przepływowi laminarnemu, a prędkość zmierza do zera przy wzrastającej odległości radialnej od lepkiego rdzenia wiru.

Обсужден класс многоячеистых вязких вихревых решений, которые в качественном отношении хорошо описывают поведение водного смерча; решения представлены аналитически при помощи внешних и внутренних разложений. Принято, что в окружающем течении не выступает осевой градиент давления. Члены высшего порядка, описывающие течение на большом расстоянии от вихря, отвечают ламинарному течению, а скорость стремится к нулю при возрастающем радиальном расстоянии от вязкого сердечника вихря.

1. Introduction

THE WATERSPOUT and its land equivalent, the tornado, are among the most violent and destructive of all atmospheric vortex flows. They are both columnar vortices and have a vertical scale of the order of 100–1000 m.

The visible part of these vortices may take on a variety of different forms. The waterspout has a highly cylindrical core and interacts with a water surface giving a cylindrical sheath of spray at the foot of the vortex. This visual similarity has led to some speculation as to how alike these two vortex structures are dynamically.

An important defining difference is the nature of the terminating surface, and many authors, e.g., BELLAMY-KNIGHTS [1], HATTON [2], RAYMOND and RAO [3], have discussed the terminating boundary conditions in detail. A waterspout is here taken to be a columnar vortex with swirling speeds of up to about 40–150 m/s lying over a body of water deep enough to exclude the effects of water-bottom. Waterspouts are more amenable to observational study than tornadoes owing to their high frequency of occurrence in certain preferred locations, for example, the Florida Keys, and also because their structure is not masked by the cloud of debris characteristic of tornadoes.

GOLDEN [4, 5] conducted a series of field experiments on waterspouts. His observations suggest that there are basic differences in the environments of tornadoes and water-

3*

spouts. For example, whereas pronounced low-level instability (c.f. Bellamy-Knights and Saci [6]) and vertical wind shear are prominent features in tornado formation, they are more typically absent from the environment of waterspouts. This supports the argument (c.f. Serrin [7]), that some atmospheric vortices can be modelled by solutions of the equations of motion without reference to the energy mechanism supporting them, particularly in the case of waterspouts and so in the analysis to follow only dynamical solutions are considered. These observations of waterspouts also suggest that near the water surface the swirl resembled closely the Rankine vortex structure of solid rotation near the axis and a potential vortex away from the axis. Waterspouts also seem almost invariably to be highly cylindrical over most of the visible core. These features suggest that the waterspout might be modelled by solutions adopting a simple variation with height.

Finally, waterspout observations appear to show a two-cell structure with a noticeably clearer central region, suggesting axial downflow, surrounded by a mistier annular outer region. This involves an axial downflow in the inner core and a sharply defined region of upflow around this core with radial inflow away from the core. This structure is an important feature of the vortex to be described in the following analysis.

2. Mathematical analysis

The energy equation will not enter the subsequent discussion as only dynamically allowable solutions of the governing equations are being sought without reference to the energy mechanisms supporting them. The assumption of incompressibility will also be made, which can be justified by considering the observed magnitudes of winds rarely exceeding 150 m/s. Axisymmetry is also assumed as observations taken throughout the life of waterspouts seem to suggest that even fairly large departures from symmetry do not affect the dynamical structure of the vortex core.

The effect of turbulence on atmospheric vortices has been discussed by, for example, Serrin [7]. The usual assumption that the eddy viscosity is constant will be adopted here. Then if ν is the sum of the kinematic viscosity and the kinematic eddy viscosity, the equations of motion reduce to laminar form.

Cylindrical polar coordinates (r, θ, z) are adopted where r is the radius, θ is the azimuthal angle and z is the axial distance, the plane $z = 0$ lying on the water surface. The velocity components in the corresponding directions are u, v, and w. The type of unsteadiness considered in this paper has a radial length scale of the order $\sqrt{\nu t}$, where t is the time. Bellamy-Knights [8] considered a similarity analysis in terms of the variable

$$(2.1) \qquad \eta = r^2/(4\nu t).$$

Then if $2\pi K$ is the ambient circulation, the velocity field

$$(2.2) \qquad u = -2\nu f(\eta)/r,$$

$$(2.3) \qquad v = -Kh(\eta)/r,$$

$$(2.4) \qquad w = zf'(\eta)/t$$

reduced the Navier–Stokes equations to the form

$$(2.5) \qquad (\eta f'' + \eta f')' + ff'' - f'^2 + C = 0,$$

$$(2.6) \qquad \eta(h'' + h') + fh' = 0,$$

a pair of coupled ordinary differential equations, where C is a constant. The boundary conditions satisfied were

$$(2.7) \qquad f(0) = 0,$$

$$(2.8) \qquad h(0) = 0$$

giving zero radial and tangential velocity on the axis. This accords with the conditions existing in a waterspout. Far away from the axis, as $\eta \to \infty$

$$(2.9) \qquad f \to \gamma\eta,$$

$$(2.10) \qquad h \to 1,$$

where γ is a constant. Hence $C = \gamma(\gamma - 1)$. This causes the velocity field to tend asymptotically to

$$(2.11) \qquad u = -0.5\gamma r/t,$$

$$(2.12) \qquad v = K/r,$$

$$(2.13) \qquad w = \gamma z/t.$$

Bellamy-Knights found analytical and numerical solutions to Eqs. (2.5) and (2.6) which were characterised by the values of γ, determining the outer potential flow and $f'(0)$ determining the axial velocity on the axis of symmetry.

Two comments should be made regarding these solutions. Firstly, they satisfy only an inviscid condition at the terminating surface, $z = 0$. Although a waterspout permits some slip over this surface, a boundary layer solution could be included as described by BELLAMY-KNIGHTS [1]. Secondly, they represent "weak" vortices in that they are driven by the outer potential flow. Mathematically, this is because u tends to infinity with increasing radius. The present work, however, shows that there exist solutions to Eqs. (2.5) and (2.6) which satisfy

$$(2.14) \qquad (u, v, w) \to (0, 0, 0) \quad \text{as} \quad r \to \infty.$$

This special case has some satisfying properties when used to model flow in a waterspout and is obtained when $\gamma = 0$, so giving a zero value of the constant in Eq. (2.5). The remaining parameter $f'(0)$ must lie in the range $-2 < f'(0) < 1$ in order to satisfy Eq. (2.14). The asymptotic behaviour of these solutions, replacing Eqs. (2.11) and (2.13), will be obtained in the next section.

3. Solution of the equations and discussion of the results

Equations (2.5) and (2.6) with $C = 0$ can be solved numerically using a modified shooting technique for which initial conditions at $\eta = 0$ are required, i.e., $f(0)$ and $h(0)$ are both zero and on the physically reasonable assumption that f and all its derivatives are

finite at $\eta = 0$, $f''(0) = A(A-1)$ where $A = f'(0)$ must be specified. A typical solution for f when $A = -1$ is shown by the curve a in Fig. 1. Alternatively, for small values of η, the solution of Eq. (2.5) may be represented by the following power series expansion:
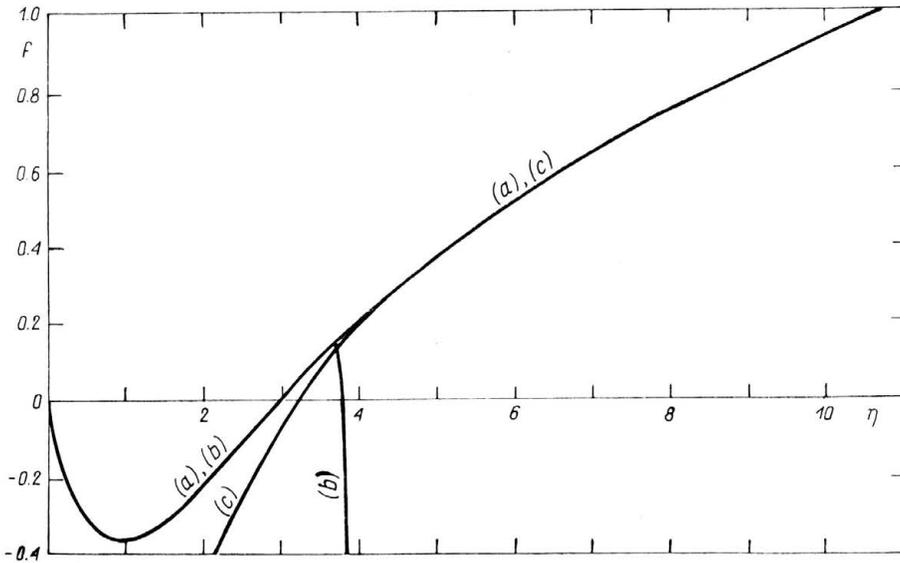
$$(3.1) \qquad\qquad f = \sum_{p=1}^{\infty} a_p \eta^p,$$

FIG. 1. Radial velocity function f versus η when $A = -1$ computed by numerical integration, the inner series expansion and the outer series expansion for curves (a), (b) and (c), respectively.

where $a_1 = f'(0)$, $a_2 = 2f''(0)$, etc. Then, substituting Eq. (3.1) into Eq. (2.5), and equating to zero successively increasing powers of η, we get for $p = 1, 2, 3, \ldots$ ad. inf.,

$$a_{p+1} = -\left\{ p^2 a_p + \sum_{q=1}^{p} q(2q-2-p) a_q a_{p+1-q} \right\} / p^2 (p-1).$$

In particular, when $p = 1$, $a_2 = 0.5 a_1 (a_1 - 1)$. Then, when A is specified, numerical computation of the series (3.1) can proceed. Curve b in Fig. 1 shows the resulting solution based on the first 100 terms of the series. The radius of convergence of the series (3.1) varies with A and is, for example, 3.6 when $A = -1.0$ and 5.1 when $A = -0.4$. It might be possible to extend the usefulness of this series by adopting methods reviewed by VAN DYKE [9]. For example, when A is positive, the signs of the coefficients a_p alternate, indicating a singularity on the negative η axis. By plotting a_p/a_{p-1} versus $1/p$, the position of the singularity can be estimated. When A is negative, the signs show a short pattern of five signs repeated with occasional slips suggesting singularities in the complex plane of η. A power series solution for h can also be obtained, i.e.,

$$h = \sum_{q=1}^{\infty} b_q \eta^q$$

where, for $q = 1, 2, 3 \dots$ ad. inf.,

$$b_{q+1} = -\left\{qb_q + \sum_{r=1}^{q}(q+1-r)a_r b_{q+1-r}\right\}/q(q+1).$$

Equation (2.6) is linear in h and so a numerical solution for any assumed nonzero value of $h'(0)$ can be normalised so that the outer boundary condition (2.10) is satisfied.

In order to determine analytically the behaviour of the solution of Eq. (2.5) for large values of η, it is useful to consider the following outer series expansion:

$$(3.2) \qquad f = c\log_e \eta + d + \sum_{i=1}^{\infty}\left(\frac{1}{\eta^i}\right)\sum_{j=0}^{i} a_{i,j}(\log_e \eta)^j,$$

where c, d and $a_{i,j}$ are constants to be determined. Substituting Eq. (3.2) into Eq. (2.5) the following explicit formula for $a_{s+1,t}$ can be obtained by equating coefficients of $(\log_e \eta)^t/\eta^{s+2}$ (for $t = s+1, s \dots 1,0$ and $s = 0, 1, 2 \dots$ ad. inf.)

$$a_{s+1,t} = \Big\{-(t+2)(t+1)a_{s+1,t+2} + 2(s+1)(t+1)a_{s+1,t+1}$$
$$-(t+3)(t+2)(t+1)a_{s,t+3}+(t+2)(t+1)(3s+2)a_{s,t+2}-(t+1)(s+1)(3s+1)a_{s,t+1}$$
$$+s(s+1)^2 a_{s,t}-c[(t+1)(t-2)a_{s,t+1}+(2s-2st-t-1)a_{s,t}+s(s+1)a_{s,t-1}]$$
$$-d[(t+2)(t+1)a_{s,t+2}-(t+1)(2s+1)a_{s,t+1}+s(s+1)a_{s,t}]$$
$$-\sum_{i=1}^{s-1}\sum_{j=0}^{i}a_{i,j}[j(2j-t-3)a_{s-i,t-j+2}+i(2i-s+1)a_{s-i,t-j}$$
$$+(js-4ij-j+i+it)a_{s-i,t-j+1}]\Big\}/(s+1),$$

where $a_{p,q}$ is zero unless $0 \leqslant q \leqslant p$ and $p \geqslant 1$. Note that there is no contribution from the double summation term in the above equation when $s = 0$ and $s = 1$. These coefficients can readily be computed given c and d. No means of deriving c and d analytically in terms of A were discovered but the validity of Eq. (3.2) was checked by obtaining c and d by matching the series solution at very large values of η with the numerically obtained solution. Then the solution given by Eq. (3.2) and retaining terms up to and including order $1/\eta^4$ compared identically with the numerically obtained solution for values of η as low as about 5.0 when $A = -1.0$ as shown by curve c of Fig. 1. The main value, however, of this outer series is that it describes analytically the behaviour of f and hence of u and w at large values of η.

i.e.

$$u = -(4\nu c\log_e r)/r + O(1/r),$$
$$w = (4\nu cz)/r^2 + O(\log_e r/r^4)$$

showing that u and w tend asymptotically to steady flow values. Moreover since $h \to 1$ as $\eta \to \infty$, $v \to K/r$ so that when $\gamma = 0$, Eqs. (2.11) and (2.13) are replaced by the above two equations but Eq. (2.12) remains unchanged. Thus the ambient flow is steady and tends to zero with increasing radius and there is no imposed axial pressure gradient. These solutions, when $\gamma = 0$, are governed by only one parameter, namely A. For $A < 0.0$ two-cell vortices are obtained whereas for $A > 0.0$ the vortices have one cell, the number

of cells being defined as one more than the number of finite zeros of f'. A further interesting feature of the present solutions is that there are no two-cell vortices with upflow on the axis. Rather, they are always characterised by downflow on the axis and radial inflow at large radial distances. This qualitatively agrees with the earlier discussed observations regarding the two-cell structure of waterspouts. Figure 2 shows $h/\sqrt{\eta}$ plotted against $\sqrt{\eta}$
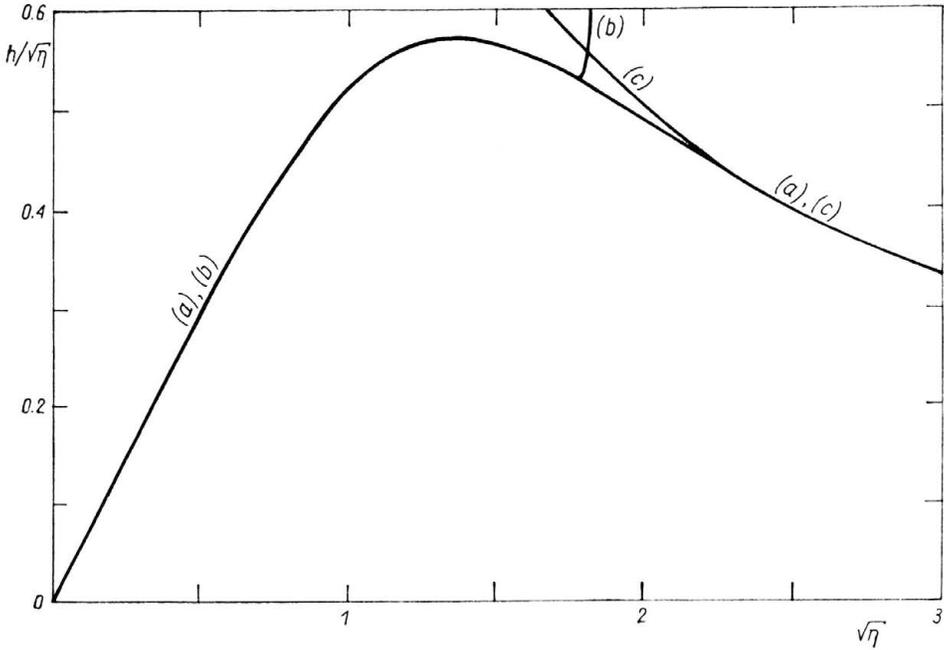

Fɪɢ. 2. Circumferential velocity function $h/\sqrt{\eta}$ versus $\sqrt{\eta}$ when $A = -1$ computed by numerical integration, the inner series expansion and the outer series expansion for curves (a), (b) and (c), respectively.

which corresponds to tangential velocity versus radius. This figure shows clearly the transition from solid rotation near the axis to the potential vortex behaviour as r increases. Thus the swirl velocity field also qualitatively agrees with observations of the Rankine like behaviour of waterspouts.

Finally it may be noted that $(v/u)^2 \to K^2/(2\nu c\log_e\eta)^2$ for large η which tends to zero as $\eta \to \infty$. Hence the formulation of Bellamy-Knights [1], which takes account of the boundary conditions at $z = 0$, could be applied.

4. Conclusions

A simple dynamical model for a diffusing waterspout is presented, which develops earlier mathematical models so that there is no imposed axial pressure gradient in the core. The resulting equations are solved numerically and analytically to give two-series expansions, valid for small and large radii respectively. The outer expansion involves loga-

rithmic terms, the leading term of which yields time independent velocity components which tend to zero with increasing radius, thus satisfying more acceptable ambient flow conditions than earlier models.

Mathematically, the present solution of the Navier–Stokes equations is an unsteady viscous diffusing vortex core embedded in a steady ambient flow which is reminiscent of the classical OSEEN [10] vortex solution. This solution, however, unlike Oseen's vortex allows radial and axial velocity in the vortex core and also shows some of the observed features of a waterspout.

Acknowledgement

References

1. P. G. BELLAMY-KNIGHTS, *An axisymmetric boundary layer solution for an unsteady vortex above a plane*, Tellus, **26**, 3, 318–324, 1974.
2. L. HATTON, *Stagnation point flow in a vortex core*, Tellus, **27**, 3, 269–280, 1975.
3. W. H. RAYMOND and G. V. RAO, *Boundary layer dynamics of a decaying vortex core*, Tellus, **30**, 5, 458–467, 1978.
4. J. H. GOLDEN, *Waterspouts and tornadoes over South Florida*, Mon. Weather Rev., **99**, 146–154, 1971.
5. J. H. GOLDEN, *The life and death of a waterspout*, New Sci., **58**, 665, 1973.
6. P. G. BELLAMY-KNIGHTS and R. SACI, *Unsteady convective atmospheric vortices*, Boundary-Layer Met., **27**, 371–386, 1984.
7. J. SERRIN, *The swirling vortex*, Phil. Trans. Roy. Soc., **A271**, 325–360, 1972.
8. P. G. BELLAMY-KNIGHTS, *Unsteady multicellular viscous vortices*, J. Fluid Mech., **50**, 1, 1–16, 1971.
9. M. VAN DYKE, *Computer-extended series*, Ann. Rev. Fluid Mech., **16**, 287–309, 1984.
10. C. W. OSEEN, Ark. Mat. Astr. Fys., **7**, 1911.

DEPARTMENT OF ENGINEERING
UNIVERSITY OF MANCHESTER, MANCHESTER, U. K.